Adiabatic heavy-ion fusion potentials for fusion at deep sub-barrier energies

S V S SASTRY, S KAILAS, A K MOHANTY and A SAXENA

Nuclear Physics Division, Bhabha Atomic Research Centre, Trombay, Mumbai 400 085, India

E-mail: snarayan@apsara.barc.ernet.in

Abstract. The recently reported unusual behaviour of fusion cross-sections at extreme sub-barrier energies has been examined. The adiabatic limit of fusion barriers has been determined from experimental data using the barrier penetration model. These adiabatic barriers are consistent with the adiabatic fusion barriers derived from the modified Wilzynska–Wilzynski prescription. The fusion barrier systematics has been obtained for a wide range of heavy-ion systems.

Keywords. Heavy-ion fusion; fusion barrier systematics; energy dependent barrier; adiabatic and sudden barriers; fusion slope function.

PACS Nos 25.70.Jj; 24.10.Eq

Heavy-ion fusion has been under intense investigation over the last two decades. Heavy-ion fusion populates compound system at high excitation energies and angular momenta, and provides a tool to study the nucleus at extreme conditions. It also opens up a new channel to generate nuclei far away from stability line and to populate the super heavy nuclei near the island of stability. Further, the fusion of heavy ions at sub-Coulomb barrier energies exhibited anomalously large enhancement over the model estimates based on tunneling of the entrance channel Coulomb barrier. This enhancement has been understood to be arising due to the strong coupling of structure of the fusing nuclei and the reaction dynamics [1]. The effects of couplings of nuclear structure on fusion have been clearly brought out in the experimental studies of the fusion barrier distributions [2] (and references therein). Nuclear fusion at extreme sub-barrier energies has been revisited recently [3,4]. Jiang *et al* [3] have reported unexpected behaviour of fusion cross-sections at extreme sub-barrier energies. The Wong's model fails to reproduce the data at these low energies. They have observed that the logarithmic slope ($L(E)$ of eq. (5)) increases with decrease of energy in contrast to a constant value expected at the deep sub-barrier energies. The failure of the Wong's model analysis to explain the unexpected behaviour of fusion of [3] is partly due to the parabolic shape of the fusion barrier assumed in the Wong's model [4]. The increase in logarithmic

47

slope with decreasing energy is also consistent with the large diffuseness parameter required to fit the high precision fusion data [4]. In the present work, we have investigated the anomalous behaviour of fusion at deep sub-barrier energies in terms of the energy dependent barrier penetration model (EDBPM) [5], and we have obtained the systematics of the lowest (adiabatic) barriers.

Fusion cross-sections at low energies decrease exponentially, reminiscent of one-dimensional barrier penetration model. This barrier is identified as the adiabatic (lowest) limit of the distribution of fusion barriers. In the present work, we identify the adiabatic region and obtain the adiabatic fusion barrier. For this purpose, we follow the barrier penetration model with an effective energy dependent barrier as discussed in [5]. In this model, at high energies (above E_2) well above uncoupled elastic channel barrier, fusion occurs by transmission through a single constant barrier known as sudden fusion barrier (V_2). As the energy decreases, the effective fusion barrier decreases linearly with energy until a lower energy (E_1) is reached. At this lower limit called adiabatic limit, fusion occurs by tunneling through a constant barrier known as adiabatic fusion barrier (V_1) [5]. The effective fusion barrier (V_{eff}), the transmission factor for fusion (T_l), the fusion cross-section (σ_f), the mean square fusion spin ($\langle L^2 \rangle$) values and the fusion slope values ($L(E)$) in EDBPM [5] are

$$V_{\text{eff}}(E) = V_2 \quad \text{for} \quad E \geq E_2,$$

$$V_{\text{eff}}(E) = \alpha E + \beta \quad \text{for} \quad E_1 \leq E \leq E_2,$$

$$V_{\text{eff}}(E) = V_1 \quad \text{for} \quad E \leq E_1, \tag{1}$$

$$\sigma_l = \frac{\pi}{k^2}(2l+1)T_l(E), \tag{2}$$

$$T_l(E) = \left[1 + \exp\left(\frac{2\pi}{\hbar\omega}(V_{\text{eff}} + V_{\text{rot}} - E)\right)\right]^{-1}, \tag{3}$$

$$\sigma_f = \sum_l \sigma_l \quad \text{and} \quad \langle L^2 \rangle = \sum_l l(l+1)\sigma_l/\sigma_f, \tag{4}$$

$$L(E) = \frac{\mathrm{d}\log(\sigma E)}{\mathrm{d}E}. \tag{5}$$

In eq. (1), $\alpha = (V_2 - V_1)/(E_2 - E_1)$ and $\beta = -\alpha E_1 + V_1$. In the above equations, the quantities R_b and $\hbar\omega$ are taken independent of energy. The sudden limit of the barrier (V_2) is generally around the one-dimensional fusion barrier, as prescribed in [6].

Wilzynski and Wilzynska showed that the adiabatic limit of the fusion barrier can be obtained in terms of the ground state masses of the fusing nuclei and the fused system [7]. In this prescription, the depth of the nucleus–nucleus (NN) potential in the adiabatic limit is given by the potential of the compound nucleus calculated with respect to the potential energy of the two separated incident nuclei of entrance channel with their Coulomb energy (C_0 in MeV) subtracted. Thus, the depth V_0 (in MeV) of a Woods–Saxon form of the NN potential in the adiabatic limit is given by $V_0 = (M_p + M_t - M_{\text{cn}})c^2 + C_0$. Recently, Wilzynska and Wilzynski modified the above prescription by considering shell correction term for the compound nucleus

[8]. The shell correction energy (S_{cn}) is taken from Moller *et al* [9]. In general, this term is found to lower the adiabatic barriers. The diffuseness parameter (a_0) of the potential can be determined by matching the first derivative of the NN potential (i.e., NN force) to that of the proximity potential at the contact distance $R_0 = R_p + R_t$. A correlation between the adiabatic barriers and the fusion energy thresholds was shown in [8] over a wide range of heavy-ion systems.

$$V_0 = (M_p + M_t - M_{\text{cn}})\,c^2 + C_0 + S_{\text{cn}}, \tag{6}$$

$$C_0 = 0.7054 \left(\frac{Z_{\text{cn}}^2}{A_{\text{cn}}^{1/3}} - \frac{Z_p^2}{A_p^{1/3}} - \frac{Z_t^2}{A_t^{1/3}} \right), \tag{7}$$

$$V_{\text{NN}}(r) = \frac{-V_0}{1 + \exp(\frac{r - R_0}{a_0})}, \tag{8}$$

$$\left. \frac{\mathrm{d}V_{\text{NN}}}{\mathrm{d}r} \right|_{r=R_0} = \frac{V_0}{a_0} = 16\pi\gamma \frac{R_p R_t}{R_p + R_t}. \tag{9}$$

In eq. (9), the surface tension coefficient and the radius parameters respectively are $\gamma = 0.9516[1 - 1.7826((N-Z)/A)^2]$ MeV/fm^2, $r_0 = 1.15$ fm [7,8]. We calculated the adiabatic barriers using these γ and r_0 for various systems listed in table 1. The diffuseness parameters of the NN potentials turn out be around 0.90–1.20 fm. Such larger diffuseness values, reported in some of the fusion studies [2], arise naturally in the prescription of adiabatic barriers. In order to verify this empirical prescription of [8] with the shell correction term, it is necessary to determine the adiabatic fusion barriers and their isotopic variation using experimental data. Therefore, we have derived the adiabatic barriers using the EDBPM fits to the experimental fusion data of some heavy-ion systems with $Z_p Z_t$ values ranging from 400 to 1100.

The best-fit parameters of EDBPM, V_1, E_1, V_2, E_2, R_b and $\hbar\omega$ values are listed in columns 5 to 10 of table 1. The experimental data for these systems are taken from [3,10–17]. These V_1 values are grossly underpredicted by the prescription of [8] with their r_0, γ values. It is observed that the values of r_0 and γ of [8] are different from the values used in nuclear data compilations of [9], i.e., $\gamma = 1.25[1 - 2.3((N-Z)/A)^2]$ MeV/fm^2, $r_0 = 1.16$ fm. Therefore, we have taken the values of r_0 and γ as well as the ground state masses and shell correction energy (E_{mic} listed in [9]). The resulting empirical adiabatic barrier parameters R_b, $\hbar\omega$ and V_{ad} are listed in columns 2–4 of table 1. These adiabatic barriers are very close to the V_1 values of column 5. The isotopic variation for a given $Z_p Z_t$ of the adiabatic barriers is also very well-reproduced. The diffuseness parameters are in the range of 0.65–0.9 fm, compared to the diffuseness values of [8] (0.8–1.2 fm). Therefore, the present $\hbar\omega$ values are slightly larger than those of [8].

Figure 1a shows the EDBPM fits to fusion cross-sections for the ^{58}Ni $+$ ^{58}Ni system in solid curves. The experimental data of [3,10] are shown by circles, showing the good quality of the model fits. The fits to fusion excitation functions for all the systems have been found to be good. In figure 1b (solid lines) we show the EDBPM fits to the fusion excitation function of ^{60}Ni $+$ ^{89}Y. The fusion of this system has been shown to exhibit anomalously steeper fall in deep sub-barrier region as compared to Wong's model estimates and coupled channels method. It can be seen that in the EDBPM, the cross-sections at deep sub-barrier region are

Table 1. Fusion barrier parameters (columns 2–4) in the adiabatic limit for various heavy-ion systems are obtained from the prescription of [8] with modified r_0 and γ values. The barrier parameters for EDBPM analysis of fusion data, V_1, E_1, V_2, E_2, R_b and $\hbar\omega$ are listed in columns 5 to 10. R_b is in units of fm and the others are in MeV.

System	R_b	$\hbar\omega$	$V_{\rm ad}$	V_1	E_1	V_2	E_2	R_b	$\hbar\omega$
^{28}Si + ^{58}Ni	9.9	3.9	52.9	52.4	51.7	54.8	57.5	9.8	3.1
^{28}Si + ^{62}Ni	10.2	3.7	51.6	50.6	49.6	54.2	57.2	11.0	2.5
^{28}Si + ^{64}Ni	10.3	3.5	50.7	49.9	49.2	54.3	58.5	10.4	2.5
^{32}S + ^{58}Ni	10.1	3.8	59.3	58.8	58.6	60.1	62.4	8.6	3.1
^{32}S + ^{64}Ni	10.6	3.4	56.5	56.5	56.0	57.8	60.2	8.3	3.7
^{36}S + ^{58}Ni	10.4	3.5	57.4	57.4	55.7	59.5	66.2	8.0	3.4
^{36}S + ^{64}Ni	10.7	3.2	55.8	55.8	53.0	56.8	59.3	8.6	2.5
^{36}S + ^{90}Zr	11.1	3.5	77.2	76.9	75.9	78.2	84.7	11.9	3.7
^{36}S + ^{96}Zr	11.4	3.2	74.8	74.5	73.5	76.7	83.9	11.9	3.7
^{40}Ar + ^{112}Sn	11.6	3.5	103.2	102.2	100.0	107.2	113.2	10.4	4.6
^{40}Ar + ^{116}Sn	11.8	3.4	102.0	102.0	100.7	106.7	110.4	10.4	4.6
^{40}Ar + ^{122}Sn	11.9	3.3	100.3	101.6	99.6	105.5	109.5	10.7	5.2
^{40}Ar + ^{144}Sm	12.0	3.5	123.6	122.6	120.6	129.1	133.4	11.9	4.0
^{40}Ar + ^{148}Sm	12.2	3.4	121.6	120.6	117.1	128.7	132.7	11.3	4.9
^{40}Ar + ^{154}Sm	12.4	3.2	119.2	116.9	113.9	128.2	132.0	11.9	5.2
^{46}Ti + ^{90}Zr	11.4	3.4	102.4	103.4	100.4	108.3	113.3	11.9	5.2
^{50}Ti + ^{90}Zr	11.5	3.3	101.7	103.4	102.2	107.3	113.8	11.9	4.3
^{46}Ti + ^{93}Nb	11.5	3.3	103.9	103.9	100.6	109.6	112.8	11.6	5.2
^{50}Ti + ^{93}Nb	11.6	3.3	103.4	103.7	101.9	107.8	110.3	11.0	3.7
^{58}Ni + ^{58}Ni	10.8	3.7	96.5	95.2	94.5	98.7	100.4	8.6	2.5
^{58}Ni + ^{64}Ni	11.3	3.3	92.5	92.8	91.3	98.9	101.9	9.8	3.7
^{64}Ni + ^{64}Ni	11.5	3.1	90.8	91.8	91.1	95.4	97.9	9.8	3.4
^{60}Ni + ^{89}Y	11.7	3.3	124.0	125.5	123.8	129.8	132.1	8.0	2.5
^{64}Ni + ^{100}Mo	12.2	3.1	127.9	130.1	128.6	139.4	142.6	11.9	3.7
^{86}Kr + ^{70}Ge	12.1	3.0	126.1	127.8	124.6	134.8	141.3	8.6	5.2
^{86}Kr + ^{76}Ge	12.2	3.0	125.4	126.9	124.6	132.6	137.4	9.2	4.9

reproduced. The best-fit values are respectively $R_b = 8.6$ fm and $\hbar\omega = 2.5$ MeV for ^{58}Ni + ^{58}Ni system and $R_b = 8.0$ fm and $\hbar\omega = 2.50$ MeV for ^{60}Ni + ^{89}Y. These values are lower than the values predicted by the prescription of [8] for these two systems. We calculated (for all systems) the exponential slope parameter $L(E)$ given by eq. (5). As shown in figures 1c and 1d, the experimental slope values are reproduced except at the lowest energies. Exact WKB transmission in place of transmission through parabolic barrier is expected to increase the theoretical model values of slope at low energy, as shown in [4]. Therefore, we have obtained fusion
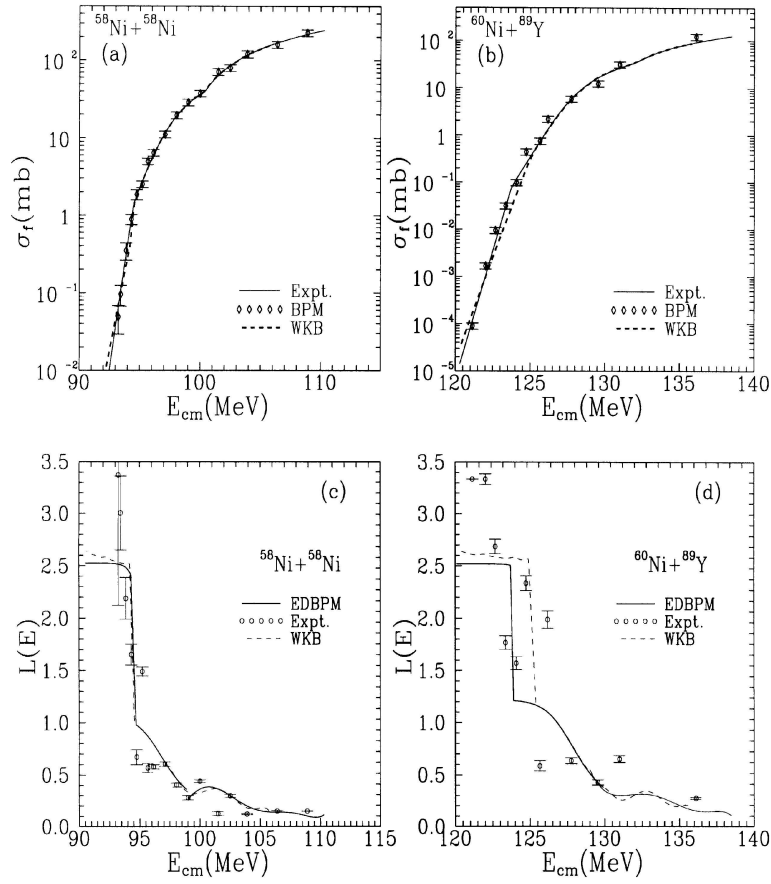
Figure 1. (**a, b**) Fusion excitation functions and (**c, d**) the fusion slope function for ^{58}Ni + ^{58}Ni and ^{60}Ni + ^{89}Y systems. The experimental data are shown by circles with error bars and the solid curves are EDBPM results.

cross-sections following WKB transmission method for lower energies ($E < E_1$). The results are shown by dashed curves in figures 1a–d. The WKB method has enhanced the fusion slope values at low energies.

The percentage deviations of adiabatic barrier heights (V_1) compared to the modified prescription of [8] have been calculated for all the systems. Further, the percentage deviations of sudden barrier heights (V_2) have also been compared to the phenomenological formulae of [6]. These are shown in figures 2a and 2b as a function of $Z_p Z_t$, which is a measure of heaviness of the system. As shown in figures 2a and 2b, the deviations of V_1 for all these systems are within 2%, whereas the deviations of V_2 are up to 6%. The solid line drawn in the figures shows general trend of $Z_p Z_t$ dependence of these deviations, obtained by a second-order polynomial fit. Even though these six parameters of EDBPM are varied independently, they exhibit strong correlations. For example, in the present study the sudden and adiabatic energies can be expressed as $E_2 = 1.00515V_2 + 3.52957$ (within ±3% accuracy) and
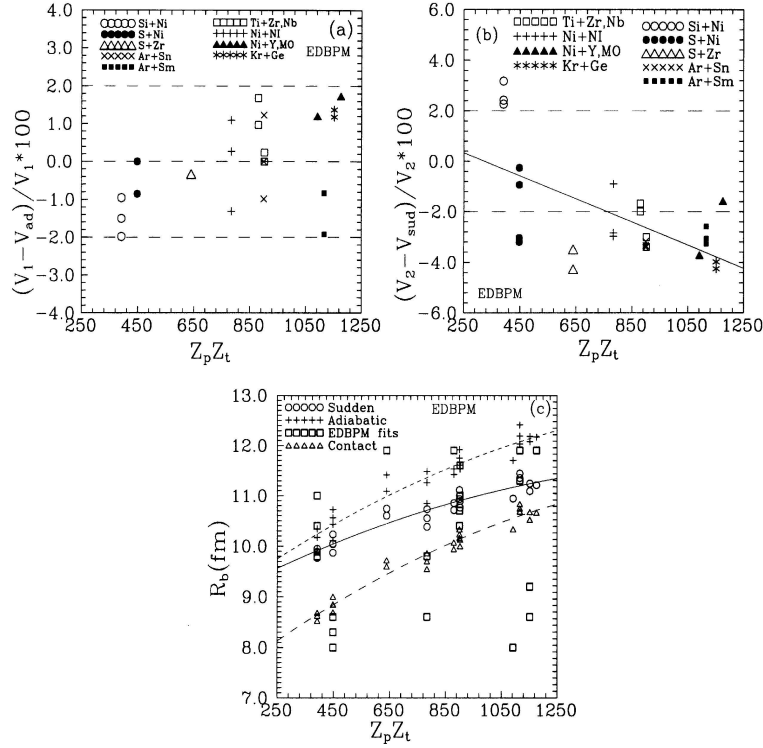
Figure 2. Percentage deviation of the (**a**) adiabatic and (**b**) sudden barriers from EDBPM method with that of empirical prescriptions. In (**c**), the fusion barrier radius values obtained from EDBPM, the corresponding sudden values from [6], the adiabatic values and the contact distance are shown for a comparison. The solid and dashed lines in figures (**a**)–(**c**) are guides to eye.

$E_1 = 0.98018V_1 + 0.111177$ (within $\pm 1.5\%$). Therefore, the sudden and adiabatic barriers (V_2 and V_1) agree very closely with the results of empirical prescriptions.

The optimised R_b values of EDBPM model (column 9 of table 1) have been plotted in figure 2c as a function of Z_pZ_t. For a comparison, the adiabatic barrier radii, the sudden values as given by [6] and the contact radii ($R_{\mathrm{con}} = 1.233(A_p^{1/3} + A_t^{1/3})$) are shown by different symbols. The solid and dashed curves are polynomial fits to data showing general trends. For some systems, the optimised R_b values are smaller than the sudden, adiabatic and contact radii values. The smallness of R_b is a requirement of the high energy fusion cross-sections for some of the systems. The $\hbar\omega$ values are important for deep sub-barrier data and are closer to the empirical adiabatic values listed in table 1. The smallness of $\hbar\omega$ is system-dependent, especially as shown for the cases of ^{36}S + ^{58}Ni and ^{58}Ni + ^{58}Ni, where fusion data extends to deep sub-barrier region. The optimised $\hbar\omega$ values for the Ar + Sm systems are around 5 MeV (see table 1) in contrast to Ni + Y system which have similar Z_pZ_t values.

In conclusion, the fusion cross-sections from well above the barrier to extreme sub-barrier energies have been analysed using the barrier penetration model. From this analysis, the adiabatic limits of fusion barriers have been determined for a wide range of heavy-ion systems. The empirical prescription of Wilzynska and Wilzynski has been used with modified radius parameter and surface tension coefficient values consistent with the parametrisation of the nuclear masses. The adiabatic fusion barriers calculated from this prescription are in good agreement with the adiabatic barriers deduced from the model fits to fusion data.

Acknowledgements

References

[1] C H Dasso, S Landowne and A Winther, *Nucl. Phys.* **A405**, 381 (1983)
[2] M Das Gupta, D J Hinde, N Rowley and A M Stefanini, *Annu. Rev. Nucl. Part. Sci* **48**, 401 (1998)
[3] C L Jiang *et al*, *Phys. Rev. Lett.* **89**, 052701 (2002)
[4] K Hagino, N Rowley and M Dasgupta, *Phys. Rev.* **C67**, 054603 (2003)
[5] V S Ramamurthy, A K Mohanty, S K Kataria and G Rangarajan, *Phys. Rev.* **C41**, 2702 (1990)
[6] L C Vaz, J M Alexander and G R Satchler, *Phys. Rep.* **69**, 373 (1981)
[7] J Wilzynski and K Siwek-Wilzynska, *Phys. Lett.* **55B**, 270 (1975)
    K Siwek-Wilzynska and J Wilzynski, *Phys. Lett.* **74B**, 313 (1978)
    J Wilzynski, *Nucl. Phys.* **A216**, 386 (1973)
[8] K Siwek-Wilzynska and J Wilzynski, *Phys. Rev.* **C64**, 024611 (2001)
[9] P Moller, J R Nix, W D Myers and W J Swiatecki, *At. Data Nucl. Data Tables* **59**, 185 (1995)
[10] M Backerman *et al*, *Phys. Rev. Lett.* **45**, 1472 (1980)
     M Backerman *et al*, *Phys. Rev.* **C23**, 1581 (1981)
[11] M Backerman *et al*, *Phys. Rev.* **C25**, 837 (1982)
[12] A M Stefanini *et al*, *Nucl. Phys.* **A456**, 509 (1986)
[13] A M Stefanini *et al*, *Phys. Rev.* **C62**, 014601 (2000)
[14] W Reisdorf *et al*, *Nucl. Phys.* **A438**, 212 (1985)
[15] P H Stelson *et al*, *Phys. Rev.* **C41**, 1584 (1980)
[16] J Halbert *et al*, *Phys. Rev.* **C40**, 2558 (1989)
[17] W Reisdorf *et al*, *Nucl. Phys.* **A444**, 154 (1985)